

DOCUMENT CONTROL SHEET

	ORIGINATOR'S REF. NLR TP 96564 U		SECURITY CLASS. Unclassified
ORIGINATOR National Aerospace Laboratory NLR, Amsterdam, The Netherlands			
TITLE Dynamics and control of a spacecraft with a moving, pulsating ball in a spherical cavity.			
PRESENTED AT			
AUTHORS J.P.B. Vreeburg		DATE 960927	pp ref 22 15
DESCRIPTORS Computerized simulation Nutation Dynamic models Rotating spheres Equations of motion Slugs Liquid sloshing Spacecraft stability Liquid filled shells Spacecraft control Motion stability Tanks (containers)			
ABSTRACT A model with two interacting bodies, for a spacecraft with liquid, has been developed. The spacecraft without liquid is the "tank" and is characterized by its inertial properties and the location and size of a spherical cavity. In the cavity is located the "slug", a sphere of uniform density with a variable radius. At the point of contact between slug and tank the interaction force and torque are prescribed as a function of liquid properties and state variables. The model is named SMS, for Sloshsat Motion Simulator. Its initial objective is to support the development of control laws for the Sloshsat spacecraft, presently under development and scheduled to be launched in 1998. Sloshsat is to perform a series of experiments for the validation of CFD models of spacecraft with onboard liquid. The SMS parameters are to be predicted by CFD simulations and finally to be validated by Sloshsat results. The special feature of SMS is the variable size of the slug. It provides a degree of freedom for the modelling of the variable shape of onboard liquid. The dynamic behaviour of SMS is illustrated and discussed for some particular cases, including a PAM-D nutation model. Control of SMS is evaluated for commanded uniform rotation about its intermediate principal axis and stabilized by a cold-gas jet system with 12 nozzles. The cavity centre is on the axis of rotation but not at the centre of mass of the tank. Although the tank is easily stabilized by its reaction control system, a very small friction between slug and tank causes angular momentum to accumulate in the slug motion and results in large oscillations of size.			

NLR TECHNICAL PUBLICATION

TP 96564 U


DYNAMICS AND CONTROL OF A SPACECRAFT
WITH A MOVING, PULSATING BALL
IN A SPHERICAL CAVITY


by

J.P.B. Vreeburg

The work described was partly carried out under a contract awarded by the European Space Agency, contract number 10416/93/NL/JG, Work Package 3055, and by the Netherlands Agency for Aerospace Programs (NIVR), contract number 2601 N.

Division : Space

Prepared : JPBV/ 

Approved : HFAR/ 

Completed : 960927

Order number : 572.401/201.536/072.022

Typ. : LMT



Contents

Introduction	5
The tank-liquid interaction problem	6
The equations of motion for a tank with liquid	7
The Sloshtat Motion Simulator SMS	9
Some validation of SMS: The PAM-D case	11
PAM-D simulation results	12
The Sloshtat reaction control system	14
Commanding of thruster activations	14
Example of a control scheme	15
A typical dynamic configuration	15
Rotation vector placement	16
Conclusions	18
References	18
14 Figures	

(22 pages in total)



This page is intentionally left blank



DYNAMICS AND CONTROL OF A SPACECRAFT* WITH A
MOVING PULSATING BALL IN A SPHERICAL CAVITY

J.P.B. Vreeburg
National Aerospace Laboratory NLR
P.O. Box 90502. 1006 BM Amsterdam, The Netherlands

A model with two interacting bodies, for a spacecraft with liquid, has been developed. The spacecraft without liquid is the 'tank' and is characterized by its inertial properties and the location and size of a spherical cavity. In the cavity is located the 'slug', a sphere of uniform density with a variable radius. At the point of contact between slug and tank the interaction force and torque are prescribed as a function of liquid properties and state variables.

The model is named SMS, for Sloshsat Motion Simulator. Its initial objective is to support the development of control laws for the Sloshsat spacecraft, presently under development and scheduled to be launched in 1998. Sloshsat is to perform a series of experiments for the validation of CFD models of spacecraft with onboard liquid. The SMS parameters are to be predicted by CFD simulations and finally to be validated by Sloshsat results.

The special feature of SMS is the variable size of the slug. It provides a degree of freedom for the modelling of the variable shape of onboard liquid. The dynamic

behaviour of SMS is illustrated and discussed for some particular cases, including a PAM-D nutation model.

Control of SMS is evaluated for commanded uniform rotation about its intermediate principal axis and stabilized by a cold-gas jet system with 12 nozzles. The cavity centre is on the axis of rotation but not at the centre of mass of the tank. Although the tank is easily stabilized by its reaction control system, a very small friction between slug and tank causes angular momentum to accumulate in the slug motion and results in large oscillations of size.

Introduction

Sloshsat FLEVO is a 100 kg spacecraft for the study of the dynamics of spacecraft with a large mass fraction of liquid in a partially filled tank. Figure 1 shows the main features in a view of the spacecraft with the solar panels removed. The launch with the US STS is planned for 1998.

The payload is an instrumented, smooth 87-litre tank filled with 33.5 litres of water. The tank cavity is a circular cylinder of

* Sloshsat FLEVO is a harmonized programme between the European Space Agency (ESA) and the Netherlands Agency for Aerospace Programs (NIVR). Main contractor is the National Aerospace Laboratory NLR (The Netherlands) with participation of Fokker Space (The Netherlands), Verhaert (Belgium), Newtec (Belgium), Rafael (Israel) and NASA (USA). The Sloshsat FLEVO development is performed in the framework of the ESA Technology Development Programme (TDP) Phase 2 and the NIVR Research and Technology (NRT) programme.

length equal to radius, capped by hemispherical domes. The empty spacecraft mass is 73 kg; its centre of mass (com) is near the equatorial plane of the tank just outside the cavity wall; its principal moments of inertia (m.o.i.) are, in kg.m²:

$I_1 = 7.8$, $I_2 = 6.5$, $I_3 = 5.8$. The axis of symmetry of the cavity is parallel to the axis of minimum m.o.i. and intersects the axis of intermediate m.o.i.

The experimental programme for Sloshtat FLEVO is defined by its Investigators Working Group (IWG) with participants from The Netherlands, U.S.A. and Israel. The experiments are classified in three categories,

- i. Hydrostatics and stability, at uniform tank rotation rate,
- ii. Settling manoeuvres, to bring the liquid at a desired location,
- iii. Spacecraft dynamics, for identification of stable transient motions

In order to size the reaction control subsystem of 12 cold-gas jets and for the preparation of the operations, a dynamic model of Sloshtat¹ has been developed. The model, named SMS for Sloshtat Motion Simulator, is depicted in figure 2 and will be described in some detail in a later section. It consists of an invariable tank body with a spherical cavity and a spherical slug of variable size to represent the liquid.

The paper discusses the main features of SMS and explores some strategies for control actions. The results of these actions on SMS are demonstrated by examples. In a previous investigation a state vector based on slug trajectory variables had been defined. The consequent set of equations to predict system evolution were highly nonlinear and did not provide much insight in system behaviour. The present, modest goal is to show the system response to simple control actions. These are to serve as building blocks for more sophisticated

control implementations, as are to be developed by the IWG members, for translation into commands by the Sloshtat onboard Data Handling Subsystem that governs the spacecraft operations.

The tank-liquid interaction problem

The flow of liquid about a closed surface generates hydrodynamic force and torque. If the surface belongs to a sufficiently light body, the force and torque may affect the attitude of the surface and so influence the flow. Examples with external flow are aircraft and boats; for internal flow consider tanker vehicles or geodynamic flows. In the sequel internal flow about a surface of invariable shape will be considered. The surface forms the cavity of a body with constant inertial properties, the tank.

The reference to vehicles already implies the technological relevance of the subject matter. However, rather than for its effect on the motion of the tank, internal liquid flow has been studied mostly to assess the impact on the structural strength of the tank. Only recently have analysis capabilities become sufficiently powerful to allow successful prediction of transient vehicular motion resulting from carried liquid.

A special case is the full tank. A famous example was studied by Lord Kelvin as the 'liquid gyrost'at², with an ellipsoidal cavity. The analysis by Greenhill showed that steady flow is possible only if the axial length is shorter than, or more than three times as long as, the equatorial diameter. He formulated the equations of motion in a coordinate system moving with the cavity, and this has been the rule also for all later analyses. There are some exceptions, for example the use of the so-called Tisserand frame for problems of deformable systems with constant angular momentum.

Terrestrial tanker vehicles often have tanks of such shape that liquid flows predominantly in two dimensions. A

Computational Fluid Dynamics (CFD) treatment of a 2-D liquid slosh problem can now be connected to a 3-D tank model and incorporated in a vehicle dynamics simulation for realistic predictions of system behaviour³. The liquid dynamics can be treated 3-D as well but the effort required is often forbidding unless the liquid motions are small⁴. Analytical approaches to the interaction problem are much rarer⁵.

On spacecraft the settling effect of terrestrial gravity is absent. A comparable influence sometimes is generated by the rotation rate of the tank; if the rate is sufficiently high and the liquid sufficiently distant from the rotation axis. A basic rotation rate is a particular feature of unsupported vehicles like spacecraft. It is often imposed to induce stability, but also to average out aerodynamic forces as for rockets. The analysis of the dynamics has no connection to that of terrestrial vehicles but may use results from rotating machinery^{6,7}.

The literature on the effects of liquid motions on spacecraft dynamics is large and cannot be discussed within the constraints of the paper.

The principal subjects are the stability of rotating spacecraft, and the control of nonrotating spacecraft, for attitude, motion and liquid fuel management. A recent paper⁸ can be used to gain entrance to the literature.

If the acceleration field in the tank is so low as to make the liquid surface tension influential, special problems arise. The CFD treatment of the free surface must be accurate or the predicted liquid configuration will soon be different from the real shape. The contact line evolution merits special attention since here the surface tension force acts on the tank. Sometimes the numerical behaviour of the calculated free surface may be quite satisfactory but the real liquid shape is still not achieved.

Sloshsat is conceived to generate results that can be verified by such calculations and so help to establish the conditions for successful prediction. Included in the experimental data will be information on the behaviour of the liquid at the contact line.

Another problem has to do with the numerical stability of the algorithms for the calculation of the system dynamics. If the liquid inertia is larger than that of the tank, special methods⁹ must be used or the calculations diverge.

Certain types of liquid-tank interaction can be studied on earth, and test rigs have been constructed^{10,11}. If surface tension effects are important, only experiments in weightlessness are satisfactory and these have been conducted already from the beginning of spaceflight^{12,13}. Data from operational spacecraft have been evaluated also¹⁴.

A precursor of Sloshsat has been the Wet Satellite Model¹⁵ experiment. It had a tank cavity between two cylinders. This annulus was narrow and so permitted to neglect the liquid velocity in radial direction. Consequently, a 2-D treatment of liquid flow was realistic. The experiment article was launched by sounding rocket and made a successful flight in weightlessness for about 370 s. In that time the tank almost completed a flat-spin transition from an initial rotation about its minimum m.o.i.

The equations of motion for a tank with liquid

The interaction force and torque between the liquid and the tank are obtained by integration of the equations of motion for the liquid. For a Newtonian liquid these are the equations of Navier-Stokes. The integration is to be performed in the coordinate system moving with the tank¹⁶. The temporal derivative of a field quantity \underline{K} in a moving coordinate system is related to the temporal derivative in an inertial system by :



$$\frac{\partial \underline{K}}{\partial t} /_{in.} = \frac{\partial \underline{K}}{\partial t} /_{mov.} - \quad (1)$$

$$[(\underline{V} + \underline{\Omega} \times \underline{r}) \cdot \nabla] \underline{K} + \underline{\Omega} \times \underline{K}$$

where subscripts in. and mov. refer to the inertial and moving space, and:

- \underline{r} = the position vector in the moving coordinate system
- \underline{V} = the velocity of the origin of the moving system
- $\underline{\Omega}$ = the rotation rate of the moving system

If \underline{u} denotes the liquid velocity with respect to the moving coordinate system, its velocity in the inertial system is $\underline{v} = \underline{u} + \underline{V} + \underline{\Omega} \times \underline{r}$.

Integration of the linear and angular momentum of elements of the compound body formed by the liquid and the tank yields the total force \underline{F} and the total torque \underline{T} that act on the system :

$$\underline{F} = m \left\{ \frac{d\underline{V}}{dt} + \dot{\underline{\Omega}} \times \underline{r}_c + \underline{\Omega} \times (\underline{\Omega} \times \underline{r}_c) \right\} + \quad (2)$$

$$\int_{V_L} \rho \left\{ \dot{\underline{u}} + (\underline{u} \cdot \nabla) \underline{u} + 2 \underline{\Omega} \times \underline{u} \right\} d\tau$$

$$\underline{T} = m \underline{r}_c \times \frac{d\underline{V}}{dt} + \underline{R} \cdot \dot{\underline{\Omega}} + \underline{\Omega} \times \underline{R} \cdot \underline{\Omega} + \quad (3)$$

$$\int_{V_L} \rho \underline{r} \times \left\{ \dot{\underline{u}} + (\underline{u} \cdot \nabla) \underline{u} + 2 \underline{\Omega} \times \underline{u} \right\} d\tau$$

where d/dt denotes differentiation in the inertial system while a superscript dot represents differentiation with respect to the moving coordinate system, and

- V_L = liquid volume
- ρ = material density

- m = system mass
- $\underline{r}_c = \frac{1}{m} \int_V \rho \underline{r} dV$ = system com location
- $\underline{R} = - \int_V \rho \underline{r}^2 dV$ = system inertia tensor about the origin of the moving coordinate system

In these definitions V is the system volume and \underline{r} denotes the skew-symmetric matrix formed from vector \underline{r} .

Equations (2) and (3) represent the so-called 'frozen liquid'¹⁷ description of the system equilibrium. The name stems from the fact that the integrals represent the momentum deficit or excess in the liquid with respect to a solid body of the same shape moving with the tank. It is noted that integration of the equations in time is generally stable.

If all liquid contributions are collected in force \underline{F}_L and torque \underline{T}_L , the equilibrium of the tank is expressed by :

$$M \left\{ \frac{d\underline{V}}{dt} + \dot{\underline{\Omega}} \times \underline{r}_z + \underline{\Omega} \times (\underline{\Omega} \times \underline{r}_z) \right\} = \quad (4)$$

$$= \underline{F}_L + \underline{F}_E$$

$$\underline{I} \cdot \dot{\underline{\Omega}} + \underline{\Omega} \times \underline{I} \cdot \underline{\Omega} = \underline{T}_E + \underline{T}_L + \quad (5)$$

$$(\underline{r}_E - \underline{r}_z) \times \underline{F}_E + (\underline{r}_L - \underline{r}_z) \times \underline{F}_L$$

where

- M = tank mass
- \underline{I} = tank inertia tensor about tank com
- \underline{r}_z = tank com location
- \underline{r}_E = external force action point
- \underline{r}_L = liquid force action point
- $\underline{F}_E, \underline{T}_E$ = external force, torque
- $\underline{F}_L, \underline{T}_L$ = liquid force, torque

The defined quantities are also indicated in figure 2.

Use of the Navier-Stokes equations for incompressible liquid allow to perform the integrations in equations (2) and (3) to yield¹⁶ :

$$\underline{F}_L = \int_{S_w} \{p\underline{n} - \mu(\underline{n} \cdot \nabla)\underline{u}\} dS + \oint_C (\sigma\underline{v} + \mu\underline{u} \times \underline{s}) d\gamma \quad (6)$$

$$\underline{T}_L = \int_{S_w} [\underline{r} \times p\underline{n} + \mu \{ \underline{n} \times \underline{u} - \underline{r} \times (\underline{n} \cdot \nabla)\underline{u} \}] dS + \oint_C \underline{r} \times (\sigma\underline{v} - \mu\underline{u} \times \underline{s}) d\gamma \quad (7)$$

where \underline{n} = the normal to wetted surface S_w
 \underline{s} = the tangent to contact line C
 $\underline{v} = -\underline{n} \times \underline{s}$
 p = liquid pressure
 μ = dynamic viscosity coefficient
 σ = surface tension

The Sloshsat Motion Simulator SMS

Although equations (6) and (7) are of interest, one still needs a solution for the fluid dynamic problem in the tank in order to get data for the integrands in the equations. Rather than generating such a solution by CFD and incur a formidable computational burden, it was decided to construct a model via semi-stationarity considerations, in analogy to such an approach to mechanics of vehicles affected by external flow. The result¹ is similar to many mechanical models for spacecraft with liquid, as evident from the available literature, except for a special feature that is discussed in the next paragraph. Like most other models, SMS is nonlinear and its parameters are not assumed but related to actual physical quantities. Thus, SMS may serve as a structure for the interpretation of experimental or CFD data and, hopefully,

can be made to fit these data for a wider range of conditions than previous constructs.

The model follows from equations (2) and (3) by substitution of the integral terms with expressions taken from stationary, kinematically similar flows. The parameters that govern the similarity are the relative rotation rate and the relative com velocity of the liquid, together with the ad hoc assumption that the liquid is coherent. The spatial extent of the liquid affects its moment of inertia tensor and thus the rotation rate since the angular momentum is likely to change only slowly. The spatial extent also determines the wetted wall area and thus the coupling with the tank. Therefore a variable liquid configuration would be required to model such phenomena. This special feature is included in SMS via a single parameter: the radius of a uniform density sphere, denoted 'slug', that models the liquid. As shown in figure 2, the slug is free to move in a spherical cavity but always contacts the wall. The dimensions of the spheres are chosen such that the liquid com moves in the correct physical space. Extensions of SMS to nonspherical shapes are feasible but will be attempted only if the present simple model is shown to be untenable. With the assumptions, the slug equations of motion become:

$$m \left[\frac{d\underline{v}}{dt} + \dot{\underline{v}} + 2\underline{\Omega} \times \underline{v} + \dot{\underline{\Omega}} \times \underline{r} + \underline{\Omega} \times (\underline{\Omega} \times \underline{r}) \right] = -\underline{F}_L \quad (8)$$

$$\frac{2}{5} m(R-r) [-2\dot{r} (\underline{\Omega} + \underline{\omega}) + (R-r) (\dot{\underline{\Omega}} + \dot{\underline{\omega}} + \underline{\Omega} \times \underline{\omega})] = \underline{T}_L - (R-r) \underline{e} \times \underline{F}_L \quad (9)$$

where

m = slug mass

R = cavity radius

$\underline{r} = r \underline{e}$ = slug centre location

$\underline{v} = \dot{\underline{r}} = \dot{r} \underline{e} + r \underline{w} \times \underline{e}$ = slug centre velocity

$\underline{w} = \underline{e} \times \dot{\underline{e}}$ = swirl = rotation rate of unit vector \underline{e}

$\underline{\omega}$ = slug rotation rate

these last four vectors represent variables relative to the moving coordinate system.

The liquid force and torque expressions are taken from experimental data in translating and rotating containers that produce similar values of the integral dynamic properties of the liquid. It is of interest to present the expression of the normal component of the interaction force that results from the assumptions that the liquid configuration is in fact spherical, that the 'breathing' motion is not damped, that the tank com is at the centre of the cavity, and that no external force acts¹ :

$$N = \frac{3(m+M)^2}{mM(3m+8M)} \frac{H_D^2}{r^3} + \frac{25M}{2m(3m+8M)} \frac{h^2}{(R-r)^3} - \frac{40\pi M}{3m+8M} \sigma(R-r) \quad (10)$$

where

H_D = angular momentum of the 'dumbbell' formed by the tank and slug point masses

h = angular momentum of the slug.

Also, this model gives a free slug a fundamental oscillation frequency intermediate between those of a drop and a

bubble of the size of the slug. That property was reason to include the model as an option in the SMS computer programme, to generate normal force magnitude. It was found to produce results not very different from those with other models for the normal force component.

The sign of the surface tension σ can be chosen to be compressive or expansive on slug size. Without expansive action from slug rotation, a compressive surface tension may reduce the slug size to zero. Therefore a lower limit is set on slug size, calculated to correspond to the minimum m.o.i. of the liquid modelled. If the slug hits this size with non-zero centre velocity, linear momentum is transferred to the tank in such amount and direction that the component of the centre velocity along this direction is reversed and has a chosen fractional magnitude. The necessary conditions on the impact result from the conservation of momentum for the system. A physical phenomenon that is similar to the process is the geyser that forms if liquid impacts on a wall.

Verification and test of SMS revealed some characteristic properties but a systematic investigation has not been performed. A remarkable finding is the tendency of SMS to settle in a state with eigenfrequencies that match the excitation frequency. Thus, when during verification testing, the reaction control system was operated at 25 Hz, SMS was found to produce a slug size with an eigenfrequency of 12.5 Hz, in agreement with an earlier found fact that the strongest liquid response is at the subharmonic. The data for the test were not Slosat properties; these do not permit a slug fundamental frequency in that range. The evaluation of flat-spin manoeuvres, i.e. the natural transfer of the motion from a rotation about the minimum m.o.i. to a rotation about the maximum m.o.i., showed an extreme sensitivity to damping. A truly minute increase in the damping of the breathing



motion of the slug was found to delay the transfer from 16 to 21 minutes for an initial spin rate of 0.4 s^{-1} .

Some validation of SMS:

The PAM-D case

The Perigee Assist Motor D is a spin-stabilized upper stage that has been used on several missions. It has been observed that near the end of the burn the system developed a growing nutation motion. A tentative explanation^{18,19} relates the instability to the effects of a pool of molten slag from the solid propellant, trapped in the aft motor chamber.

SMS should be able to simulate the PAM-D behaviour provided that the inertial properties of its constituent bodies are made variable with time. The possibility to prescribe a thrust (or a torque) was already included in SMS.

The required extension of SMS identifies a piece of material of mass μ and inertial tensor \underline{I} that has its com located at \underline{p} . This material is taken from the tank and allocated to the slug (or vice versa) such that momenta are conserved and the system com is not changed. Thus consider the system of three bodies:

	mass	inertia tensor	com location	inertial velocity	rotation rate
transfer material	μ	\underline{I}	\underline{p}	$\underline{v} + \underline{\Omega} \times \underline{p}$	$\underline{\Omega}$
tank	$M - \mu$	\underline{I}'	\underline{z}'	$\underline{v} - \underline{\Omega} \times \underline{z}'$	$\underline{\Omega}$
slug	m	$\frac{2}{3}m(R-r)^2 \underline{I}$	\underline{z}	$\underline{v} + \underline{\Omega} \times \underline{p} + \underline{v}$	$\underline{\Omega} + \underline{\omega}$

The configuration is illustrated in figure 3. If μ is allocated to the tank there results a body with mass M , com location \underline{z} , whence

$$\underline{z}' = \frac{1}{M - \mu} (M \underline{z} - \mu \underline{p}) ,$$

$$\text{inertia tensor } \underline{I} = \underline{I}' + \underline{I} - \frac{\mu(M - \mu)}{M} \{ \underline{p} - \underline{z}' \}^2 ,$$

velocity $\underline{v} + \underline{\Omega} \times \underline{z}$ and rotation $\underline{\Omega}$

where $\{ \underline{p} - \underline{z}' \}$ is the skew-symmetric matrix formed from vector $\underline{p} - \underline{z}'$. If μ is allocated to slug m its mass changes to $m + \mu$, and new values \underline{I}' , $\underline{\omega}'$ and \underline{v}' replace the values of these vectors without quote. The value of \underline{I}' is made determinate by the condition that μ is distributed along a negligibly thin ring on a sphere of radius R about the origin C of the coordinate system fixed to the tank.

The new values follow by straightforward algebra and are not reproduced here except for the relative velocity of the slug:

$$\underline{v}' = \frac{m}{m + \mu} \underline{v} \tag{11}$$

This equation is important since it expresses the fact that the mass transfer effects a decrease of the velocity of the slug with respect to the tank, i.e. friction. The presence of friction will be required later in the paper.

Although the reallocation of mass from tank to slug involves momentum transfer, it is not necessary to consider the details. As shown next, the evolution of the system state can be realized directly with the integration algorithm.

For SMS, the state differential equation $\dot{y}' = F(x,y)$ is integrated with time step h using a Runge-Kutta-4 formula:

$$y_{n+1} = y_{n+1/2} + \frac{1}{6}(2k_2 + k_3) \tag{12}$$

where subscript n denotes the value at time nh , and

$$k_0 = h F(x_n, y_n) ,$$

$$k_1 = h F(x_n + \frac{1}{2}h, y_n + \frac{1}{2}k_0) ,$$

$$k_2 = h F(x_n + \frac{1}{2}h, y_n + \frac{1}{2}k_1) ,$$

$$k_3 = h F(x_n + h, y_n + k_2) ,$$



A basic assumption is:

$$F(x_n + \alpha h, y_n + k) = f_n(y_n + k) + p_{n+\alpha} \quad (13)$$

where f_n denotes \dot{y} of the system with invariable inertia while $p_{n+\alpha}$ represents the additional term that accounts for the effects of the reallocation of material.

Substitution of equation (13) in the expression for $y_{n+\frac{1}{2}}$ yields:

$$y_{n+\frac{1}{2}} = \frac{1}{3} [y_n + \frac{1}{2} h f_n(y_n) + \frac{1}{2} h p_n] + \frac{2}{3} [y_n + \frac{1}{2} h f_n \{ y_n + \frac{1}{2} h f_n(y_n) + \frac{1}{2} h p_n \} + \frac{1}{2} h p_{n+\frac{1}{2}}] \quad (14)$$

If one denotes by z_n the value of y_n for $f_n = 0$, i.e. using only p_n , equation (14) gives:

$$z_{n+\frac{1}{2}} = y_n + \frac{1}{2} h (\frac{1}{3} p_n + \frac{2}{3} p_{n+\frac{1}{2}})$$

Suppose that $p_n = p_{n+\frac{1}{2}}$ is a realizable condition, a very mild assumption, then:

$$z_{n+\frac{1}{2}} = y_n + \frac{1}{2} h p_n$$

and it is noted that $z_{n+\frac{1}{2}}$ can be calculated immediately from the conservation laws, as explained before, without knowledge of p_n . Define $Y_{n+\frac{1}{2}} = z_{n+\frac{1}{2}} + \frac{1}{2} h f_n(y_n)$, then

substitution in (14) provides:

$$y_{n+\frac{1}{2}} = z_{n+\frac{1}{2}} + \frac{1}{6} h [f_n(y_n) + 2 f_n(Y_{n+\frac{1}{2}})] \quad (15)$$

Progression to y_{n+1} is achieved similarly and the modified Runge-Kutta algorithm has been incorporated in SMS. The test runs showed correct evolution of momenta and kinetic energies.

PAM-D simulation results

The configuration of PAM-D in the SMS framework is sketched in figure 4. The data are inferred from the descriptions in references 18 and 19. Point C is the origin of the SMS coordinate system and the centre of a cavity with radius that was set initially at 0.61 m. This radius gives the correct location and dimensions of the ring-shaped volume that holds the molten slag on PAM-D. The size of this ring is determined by an angle $\alpha=23.6^\circ$. The minimum radius of the SMS slug representing the liquid is, rather arbitrarily, put at 0.1m. It is found that the slug angular momentum keeps the slug at a larger size, notwithstanding the PAM-D thrust of 71400 N.

Point D represents the com of the solid part (of the 'tank') and moves uniformly from its initial to its final location on the axis of symmetry during the 85s of the burn. The remaining inertial properties of the tank are:

initial mass = 3252.9 kg, decreasing with 23.673 kg/s
axial m.o.i. = 716.8 kg m², decreasing with 4.0153 kgm²/s
transverse m.o.i. = 2901.6 kg m², decreasing with 24.98 kgm²/s

The slug mass increases with 0.308 kg/s from an initial value of 1.02 kg. All rates are zeroed after 85 s (end of burn). The tank initial rotation rate is $2\pi/s$ about its axis of symmetry; the slug initially rotates with tank rate.

The location of the exit plane is relevant for the calculation of the jet damping moment.

This effect, together with a term $\dot{\underline{i}} \cdot \underline{\Omega}$ to form the Coriolis moment, has been included in the SMS model but did not lead to results substantially different from results without the effect. In figure 5 are shown the evolution of the angle between the initial and the current direction of the PAM-D axis of symmetry. The second curve is for a value of $\alpha=59.7^\circ$ and viscous friction in the slug. The curves are essentially the same, and it has been found generally that neither α -value nor viscous friction has an influence.

The evolution of the slug size for the configuration with $\alpha=23.6^\circ$ and no viscous friction is displayed in figure 6. Viscous friction does strongly affect slug size. The physical explanation is that it reduces slug rotation but is not very effective in reducing the slug com velocity relative to the tank since this velocity is small. In figures 7 and 8 are shown in one plot the evolution of a component of the PAM-D nutation rate and a component of the slug direction vector. In figure 8 the tank diameter is taken 0.41 m and it is seen that this parameter has a strong effect on the growth rate of the nutation rate. The tank diameter controls the magnitude of the force that centers the slug at the 'lowest' point in the tank. Clearly phase lock has occurred between nutation rate and slug motion while frequencies are different.

A stability analysis of PAM-D using the SMS model would require more space than available in this contribution. Nevertheless, a simple criterion, due to Poincaré and discussed in reference 20, has been found that correctly predicts the onset of the nutation divergence. To be investigated is the stability of the 'dumbbell' formed by the com's of the solid and liquid parts of PAM-D, along its nominal flight directory.

In figure 9 \underline{k} is the direction of the PAM-D trajectory in inertial space while \underline{e} is the direction of the dumbbell separation bar.

The motion of \underline{e} in inertial space is (see figure):

$$\frac{d\underline{e}}{dt} = -\dot{\varphi} \sin \theta \underline{\tau} + \dot{\theta} \underline{\tau} \times \underline{e}$$

The angular momentum \underline{H}_D of the dumbbell with respect to its com is:

$$\underline{H}_D = -\frac{mM}{m+M} \ell^2 \underline{e} \times (\underline{e} \times \underline{\Omega})$$

$\underline{\Omega} = \omega_c \underline{e} + \underline{e} \times \frac{d\underline{e}}{dt}$ =dumbbell rotation rate, m = liquid mass, M = solid mass and ℓ = dumbbell separation distance.

Consequently, the dumbbell rotational energy $T_o = \frac{1}{2} \underline{\Omega} \cdot \underline{H}_D$ is

$$T_o = \frac{1}{2} \frac{mM}{m+M} \ell^2 \left(\dot{\theta}^2 + \dot{\varphi}^2 \sin^2 \theta \right)$$

On the nominal trajectory, the thrust F is equivalent to a gravity field of strength $F/(m+M)$, whence the potential energy of the dumbbell in this field equals:

$$V = -m \frac{F}{m+M} \ell \cos \theta$$

According to Poincaré the dumbbell motion is stable if 'kinetic potential':

$$V - T_o = -m \frac{F}{m+M} \ell \cos \theta -$$

$$\frac{1}{2} \frac{mM}{m+M} \ell^2 \left(\dot{\theta}^2 + \dot{\varphi}^2 \sin^2 \theta \right) = \text{minimum,}$$

provided that there is friction between the dumbbell and its support. The latter



condition is satisfied, see equation (11), so that the criterion should be applicable.

Hence, $\theta=0$ is a stable state only if $\dot{\phi}^2 < \frac{F}{M\ell}$. The values of ϕ and the nutation frequency for the solid part of PAM-D are plotted together in figure 10. The intersection is around 54" since the burn started.

Although the present analysis is very cursory, the results substantiate the hypothesis in reference 18, viz. the nutation is generated by a jet damping effect and a pool of molten slag. However, it is to be noted that the momentum involved in the damping effect is not exhausted in the jet but conserved in the slag.

The generation of a nutation angle starts already much earlier than at 54". This is probably due to the coupling between the nutation and the slag eigenfrequencies. SMS simulations with a viscous slag showed nutation to occur via this mechanism but no dramatic divergence was observed.

The Slosat reaction control system

The SMS software has been expanded with a subroutine that models the reaction control system of Slosat, and with control subroutines that, on the basis of ideal measurements of the tank motion, specify the force and torque to be generated by the cold-gas jets. A typical control subroutine is discussed in the next section.

A coordinate system Cxyz (Fig.2) is introduced with its origin at the geometric centre of the tank, x along the tank axis of symmetry, which is also the axis of minimum m.o.i., and the axes y and z parallel to the other principal axes of inertia of the tank. In this coordinate system the tank com is located at position, in metres, (0.02,0.0,-0.27) and the axis of maximum tank m.o.i. is parallel to the y-axis.

Hardware

The nozzles of the cold-gas reaction system are shown in figure 1. They are located four in each of three orthogonal planes that intersect at an average location for the system com. Thus, in each plane, activation of two parallel jets generate a translation force while two diagonally positioned jets create a torque. Each jet has a nominal thrust of 0.88 N.

The force and torque about the geometric centre C of the tank from each thruster activation is combined in a 6 x 12 matrix:

$$\begin{bmatrix} -0.88 & 0.88 & -0.88 & 0.88 & 0.0 & 0.0 & 0.0 & 0.0 & 0.0 & 0.0 & 0.0 & 0.0 \\ 0.0 & 0.0 & 0.0 & 0.0 & -0.38 & 0.38 & -0.38 & 0.38 & 0.0 & 0.0 & 0.0 & 0.0 \\ 0.0 & 0.0 & 0.0 & 0.0 & 0.0 & 0.0 & 0.0 & 0.0 & -0.88 & 0.88 & -0.88 & 0.88 \\ 0.0 & 0.0 & 0.0 & 0.0 & 0.244 & -0.244 & -0.346 & 0.346 & 0.0 & 0.0 & 0.0 & 0.0 \\ 0.125 & -0.125 & 0.125 & -0.125 & 0.0 & 0.0 & 0.0 & 0.0 & 0.319 & -0.319 & -0.319 & 0.319 \\ 0.22 & -0.22 & -0.22 & 0.22 & 0.0 & 0.0 & 0.0 & 0.0 & 0.0 & 0.0 & 0.0 & 0.0 \end{bmatrix} \quad (16)$$

Multiplication of this matrix by a column vector with 12 'on' (=1) or 'off' (=0) commands yields the components of the total force and torque on the system. The total force components along axes x, y and z are in the first three entries of the 6-component column vector that results from the multiplication, the torque components in the last three.

Commanding of thruster activations

Suppose the requirement has been calculated to generate an amount of linear momentum \underline{L} N.s and angular momentum \underline{H} N.m.s. One standard interval Δt of thruster activation generates contributions to the linear and angular momentum components equal to the entries in matrix (16) multiplied by Δt . In order to determine the number of activations for each thruster, the pseudo-inverse of matrix (16) is multiplied with the required linear and angular momentum components aggregated in a

6-component column vector. The outcome is a 12-component command vector.

To be specified is the number of thruster activations allotted for realization of the command vector. If this number is smaller than the largest positive component of the vector, the vector is scaled such that this component becomes equal to the number.

During the sequence of allotted thruster activations, a particular thruster is commanded 'on' if its entry in the command vector is larger than 0.5. After each standard interval the command vector components are reduced by the figure that was realized during the interval, and the activations for the next interval decided. Note that the activation of a thruster generates torque components along more than one direction and so influences the commands to the other thrusters in the next interval.

A more efficient use of thruster gas was achieved when the command vector was multiplied with a positive number less than one before the activation sequence is determined, although it then takes longer before a control objective is satisfied. This simple approach to control implementation worked satisfactory, but is likely to require refinement for more sophisticated control objectives.

Example of a control scheme

The specification of the momenta that are to be realized by the reaction control system is based on a control law that seeks to achieve a desired state of the system. Sequencing of different control laws is planned for the realization of complex manoeuvres. It is part of the preparation for Sloshtat operations to identify the 'building blocks' of such manoeuvres. Discussed will be a control to achieve a desired rotation rate of the tank.

The application of force and torque will be accounted for by the addition of small amounts of momentum to the momentum vectors of the tank. It is assumed that these vectors are constant at the values measured just before the application. The activation periods must therefore be small with respect to characteristic timescales of the tank motion.

The analyses in the sequel will use projection matrix $\underline{\underline{P}}$ of the form: $-\underline{k}^2$, where \underline{k} is a unit vector. For matrix $\underline{\underline{P}}$ this vector is along the vector $\underline{e} \times \underline{r}_z$ and consequently:

$$\underline{\underline{P}} \cdot \underline{e} = \underline{e}, \quad \underline{\underline{P}} \cdot \underline{r}_z = \underline{r}_z,$$

$$\underline{\underline{P}} \cdot (\underline{e} \times \underline{r}_z) = 0$$

Operation of $\underline{\underline{P}}$ on a vector \underline{A} yields its components along \underline{e} and \underline{r}_z

$$|\underline{e} \times \underline{r}_z|^2 \underline{\underline{P}} \cdot \underline{A} = -[(\underline{e} \times \underline{r}_z) \cdot (\underline{r}_z \times \underline{A})] \underline{e} +$$

$$+ [(\underline{e} \times \underline{r}_z) \cdot (\underline{e} \times \underline{A})] \underline{r}_z =$$

$$= (\underline{e} \cdot \underline{A}) \underline{r}_z \times (\underline{e} \times \underline{r}_z) - (\underline{r}_z \cdot \underline{A}) \underline{e} \times (\underline{e} \times \underline{r}_z). \quad (17)$$

A typical dynamic configuration

Since the viscous friction force and torque are generally orders of magnitude smaller than the pressure force, only the normal force on the tank will be considered in the control calculations. For the SMS the pressure point is at the point of contact between slug and cavity, and so the normal force is directed along vector \underline{e} .

The results are demonstrated for a SMS cavity radius of 0.352 m. The slug radius is frozen at 0.24 m but allowed to decrease very slowly to a definite minimum at 0.22 m. These data span the range of inertial



property values that may be assumed by the liquid in the Sloshtat tank. The liquid surface tension is taken compressive and equal to 0.05 N.m⁻¹.

The normal force is modelled¹ as expressed in equation (10), only now the tank rotation rate is coupled in also since the tank com is not at the origin of the coordinate system. The initial location of the slug is (0.08,0.0,0.07); its initial velocity is (0.0,0.02,-0.02), with rotation rate about the x-axis of 0.2 s⁻¹. The tank initial rotation rate is about axis y, also with magnitude 0.2 s⁻¹. The initial conditions are denoted collectively by 'Motion 1'; a consequent data is the Weber number that comes out with a value of about 10. The natural evolution of this motion during the first minute is illustrated in figure 11. To be noted are the discontinuous jumps in the angular rate components early in the evolution. These result from impacts of the slug with the tank. The slug is essentially frozen after t = 7s, and is seen to stay in the tank half with positive z-coordinates; opposite to the half where the tank com is.

In the sequel Motion 1 will constitute the initial condition for control. The jet activation rate is set at 30 Hz while new thruster commands are calculated at a rate of 3 Hz. Thus, at each calculation the command vectors for ten activations are determined. The last of the ten periods commands no thruster activations so that the motion measurement subsystem may yield the dynamic data for the tank without thruster effects, in order to calculate the next set of command vectors. This means that the measurements must be accomplished in the 30 Hz period, or more periods will be unavailable for thrust application.

Rotation vector placement

The objective for the control scheme is to achieve a tank rotation rate of specified magnitude and direction in the body-fixed coordinate system Cxyz. The selection is

limited to equilibrium states that, once reached, would need thruster activations for stabilization only. Thence, the slug must not exert a torque on the tank which means that the contact force must be directed along the location vector of the tank com. For the present case the consequence is a slug centre location on the z-axis.

For the stated assumptions on interaction, equation (5) becomes :

$$\underline{I} \cdot \dot{\underline{\Omega}} + \underline{\Omega} \times \underline{I} \cdot \underline{\Omega} = \underline{T}_E - \underline{r}_z \times (\underline{F}_E + N\underline{e}). \quad (18)$$

Multiplication of equation (18) by matrix \underline{P} removes the term with N:

$$\underline{P} \cdot (\underline{T}_E - \underline{r}_z \times \underline{F}_E) = \underline{P} \cdot (\underline{\Omega} \times \underline{I} \cdot \underline{\Omega}) + \underline{P} \cdot \underline{I} \cdot \dot{\underline{\Omega}} \quad (19)$$

Application of control torque $\underline{T}_C = \underline{P} \cdot \underline{T}_E$ for Δt seconds generates $\underline{\delta\Omega} = \underline{\Omega}\Delta t$, whence

$$\underline{P} \cdot \underline{I} \cdot \underline{\delta\Omega} = \underline{T}_C \Delta t - \underline{P} \cdot (\underline{\Omega} \times \underline{I} \cdot \underline{\Omega}) \Delta t \quad (20)$$

The final desired state is specified by $\underline{\Omega} = \underline{\Omega}_0$ and then also

$$\underline{H} = \underline{I} \cdot \underline{\Omega} = \underline{I} \cdot \underline{\Omega}_0 = \underline{H}_0. \text{ Thus, for}$$

$$\underline{\Delta\Omega} = \underline{\Omega}_0 - \underline{\Omega}, \text{ and } \underline{\Delta H} = \underline{H}_0 - \underline{H}, \text{ the}$$

desired state is characterized by

$$\underline{\Delta\Omega} = \underline{\Delta H} = 0.$$

The control brings the tank closer to the desired state if

$$\frac{\delta H}{\delta \Omega} = \underline{I} \cdot \frac{\delta \Omega}{\delta \Omega} = \alpha \underline{\Delta H} \quad \text{and} \quad \frac{\delta \Omega}{\delta \Delta \Omega} = \beta \underline{\Delta \Omega} \quad \text{where } 0 < \alpha, \beta < 1.$$

Not all specified control torques can be made equally good by the reaction control system. It may therefore be advantageous to select the optimal torque with exploitation of the freedom in the selection of α and β . For now is chosen to control an average value, whence

$$\underline{T}_c = \underline{P} \cdot (\underline{\Omega} \times \underline{I} \cdot \underline{\Omega}) + \text{const. } \underline{P} \cdot (\underline{\Delta H} + \underline{I} \cdot \underline{\Delta \Omega}) \quad (21)$$

where the const. value remains to be selected.

As an example is calculated the forced transfer from Motion 1 to a uniform rotation of 0.25 rad.s^{-1} about the tank axis of intermediate m.o.i., the z-axis. The final state is unstable but is easily stabilized by the control system. Compared have been three control implementations c-1, c-2, c-3 that differ in the choice of the value of the const. in equation (21). The results illustrate the profound influence of the slug motion on the system dynamics, and the consequent large potential for analysis.

Control c-1 is relatively weak and requires about 20 th.s during the first minute to transfer the tank to the specified rotation rate and keep it there. The unit th.s represents the gas consumed during one second of continuous operation of one thruster.

The const. for control c-2 is about four times larger than for c-1 and the control consumes about 35 th.s in the first minute. The excursions from the nominal equilibrium conditions are much smaller than for control c-1. Control c-3 has the low value of c-1 during the first 11 s., i.e. during the time that the cosine of the angle between the actual and the target tank angular rate vectors is less than 0.9, and the high value of c-2 during the rest of the time. Gas consumption is only marginally less than for c-2. The performance is not significantly better than for control c-1, so the extra gas

consumed during this first minute of operation has not been very useful.

The evolution of the motion under control c-2 merits closer investigation. In figure 12 is shown the development of the angular momentum, in inertial space, of the dumbbell formed by the com's of tank and slug.

It is noted that the angular momentum is practically zero, i.e. the rotation vector is aligned with the separation vector between the masses and so one expects the slug to sit spinning on the z-axis. This is an important finding since it illustrates the possibility to bring the slug to a stop with respect to the tank even without the benefit of friction.

The development of the system kinetic energy shows an almost monotonous decrease after an initial rise, to a value that is realized also by the other controls. However these do not accomplish a continuous decrease; in fact both include a relative peak in system kinetic energy around $t = 30 \text{ s}$. By c-2 also the dumbbell kinetic energy is reduced to zero and the decrease of either energy value might turn out to be a suitable control criterion for bringing the slug to a stop.

A plot of the evolution of the slug location in the tank shows that indeed control c-2 puts the slug near the z-axis but on the negative side. The dumbbell has a minimal size and so the system is not in a state of minimum energy. The slug could possibly be kept at the spot by imposing a small thrust on the tank along the z-axis.

Continuation of the simulation showed that the slug started to move again and did not stay on the negative z-axis. Extension of the simulation to 1000" showed a profound influence of friction. For no friction, no remarkable behaviour was observed; control c-2 maintained the rotation about the intermediate axis without transferring energy to the system. When a small (contact line)

friction of 0.001 N was imposed to act counter to the slug translation velocity, the control was seen to pump energy into the system, i.e. in the slug kinetic energy, see figure 13. This energy resided in slug oscillation modes, as is apparent from a graph of the slug radius, figure 14. The result illustrates once more the destabilizing effect of friction in rotating systems.

Conclusions

The modelling of liquid behaviour by a variable size spherical slug proved to be fruitful. The extra degree of freedom made the system very susceptible to energy transfer between oscillation modes, a feature absent from the traditional models with fixed-length pendulums.

Although validation of SMS is not finished, it is encouraging that the behaviour of PAM-D is modelled so well. The necessary extensions to SMS before it could model PAM-D allow it to be used wider and increase validation opportunities.

Control of Sloshsat, as learned from SMS simulations, is likely to require different algorithms for manoeuvres and for maintenance of unstable equilibrium states.

References

1. Vreeburg, J.P.B., The Sloshsat Motion Simulator (SMS) and its simplifications. Proc. CEAS Symp. 'Making it REAL', Oct.30 - Nov.1, Delft, NL, Paper SpS03, with correction of figure 10.
2. Gray, A., A treatise on gyrostatics and rotational motion. Dover, New York, NY, 1959.
3. Sankar, S., Ranganathan, R., Rakheja, S., Impact of Dynamic Fluid Slosh Loads on the Directional Response of Tank Vehicles. Vehicle System Dynamics, Vol.21, 1992, pp.385-404.
4. Limarchenko, O.S., Behavior of a system of a cylindrical tank-fluid with a free surface under complex dynamic loading. PMM, Vol.23, No. 3, 1987, pp.304-309.
5. Lui, A.P-C., Lou, J.Y.K., Dynamic coupling of a liquid-tank system under transient excitations. Ocean Engng. Vol.17, No.3, 1990, pp. 263-277.
6. Gans, R.F., Yalisove, S.M., Observations and Measurements of Flow in a Partially-Filled Horizontally Rotating Cylinder. ASME paper 81-WA/FE-21, Nov. 1981.
7. Holm-Christensen, O., Trager, K., A Note on Rotor Instability Caused by Liquid Motions. J. Appl. Mech. Vol.58, 1991, pp.804-811.
8. Enright, P.J., Wong, E.C., Propellant Slosh Models for the Cassini Spacecraft. AIAA paper 94-3730-CP, 1994.
9. Vogels, M.E.S., A numerical method for the simulation of liquid-solid body dynamics. Proc. 12th World Congress on Scientific Computation, IMACS 1988, July 18-22, Paris, F.
10. Gledzer, Ye.B., Novikov, Yu.V., Estimation of the characteristics of nonstationary fluid motion in an ellipsoidal cavity on the basis of the measurement of the moments of force. Izv. Atm. Ocean. Phys., Vol.9, No.10, 1973, pp.615-617.
11. Flugrad, D.R., Obermaier, L.A., Computer Simulation of a Test Rig to Model Sloshing in Spin-Stabilized Satellites. J. Dyn. Syst. Meas. Contr., Vol.114, 1992, pp.689-698.
12. Vreeburg, J.P.B., Summary Review of Microgravity Fluid Science Experiments. NLR MP 86065 L; also ESA report, Nov. 1986, Paris, F.
13. van Schoor, M.C., Crawley, E.F., Nonlinear Forced-Response Characteristics of Contained Fluids in Microgravity. J. Spacecr. Rock., Vol.32, No.3, 1995, pp.521-532.
14. Rangarajan, S., Novel experiences with INSAT-1B operations. Adv. Astron. Sci., Vol.84, Pt.2, 1993, pp.989-1002.
15. Vreeburg, J.P.B., The Wet Satellite Model experiment. Final Reports of Sounding Rocket Experiments in Fluid



- Science and Material Sciences. ESA SP-1132, Vol.4, Oct. 1994, pp.9-21.
16. Vreeburg, J.P.B., Free Motion of an Unsupported Tank that is Partially Filled with Liquid. Proc. IUTAM Symp. Microgravity Fluid Mechanics, Bremen, D, Sep.2-6, 1991, pp.519-528.
 17. Gantmakher, F.R., Levin, L.M., The flight of uncontrolled rockets. Pergamon, 1964.
 18. Or, A.C., Challoner, A.D., Stability of Spinning Spacecraft Containing Shallow Pool of Liquid Under Thrust. J. Guid.Contr. Dyn. 17 (1994) 5, 1019-1027.
 19. Or, A.C., Rotor-Pendulum Model for the Perigee Assist Module Nutation Anomaly. J.Guid.Contr.Dyn. 15 (1992) 2, 297-303
 20. Lamb, H., On kinetic stability. Proc.Roy.Soc. A, London, 80 (1907) 168-177.

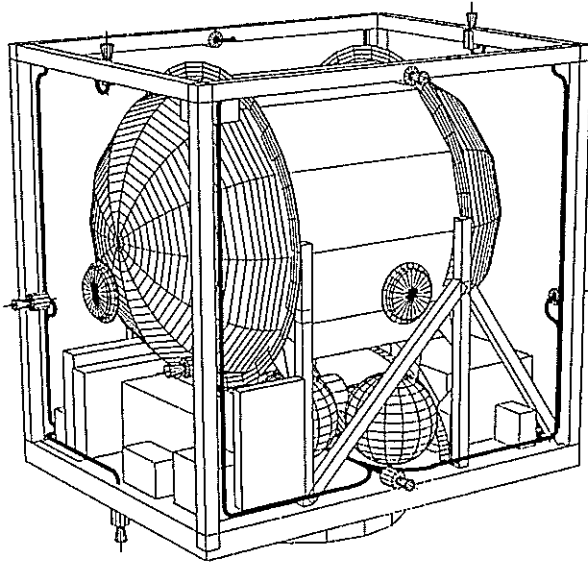


Fig. 1 Sloshtat FLEVO architecture

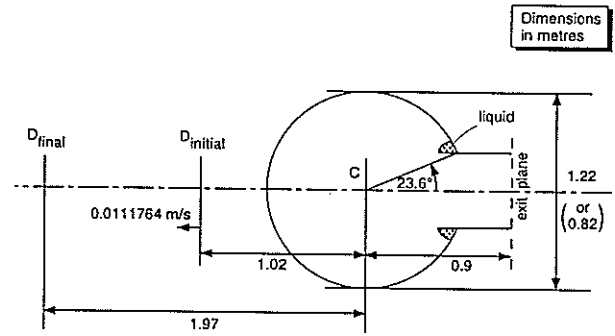


Fig. 4 Geometry of the PAM-D configuration

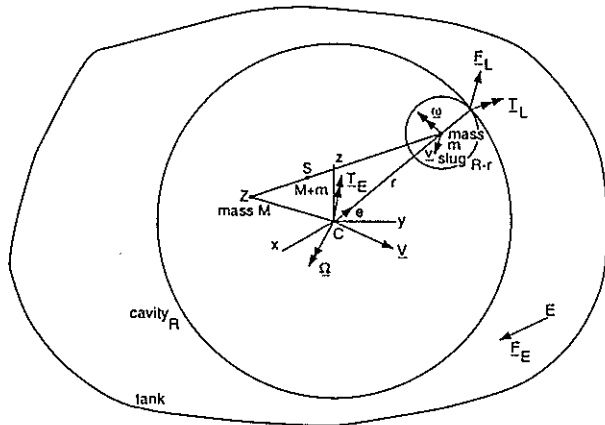


Fig. 2 The tank and slug dynamic system

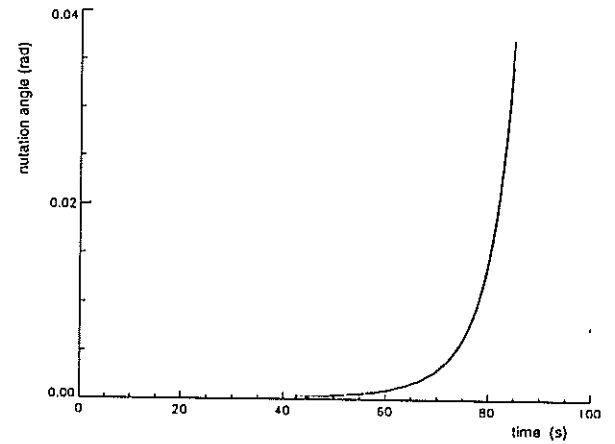


Fig. 5 Nutation angles predicted for PAM-D for different locations of the viscous, or inviscid, slug collector; tank radius 0.61 m

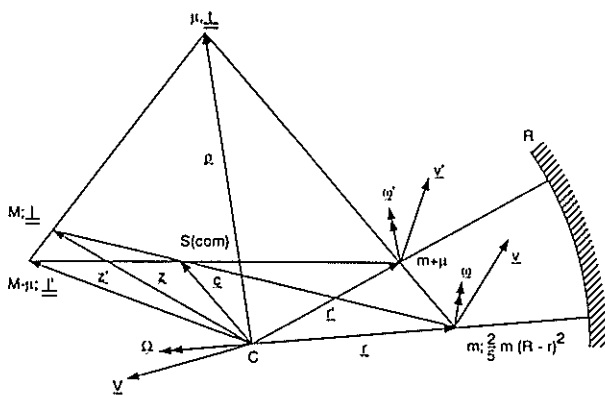


Fig. 3 System configuration for material μ allocated to either tank or slug

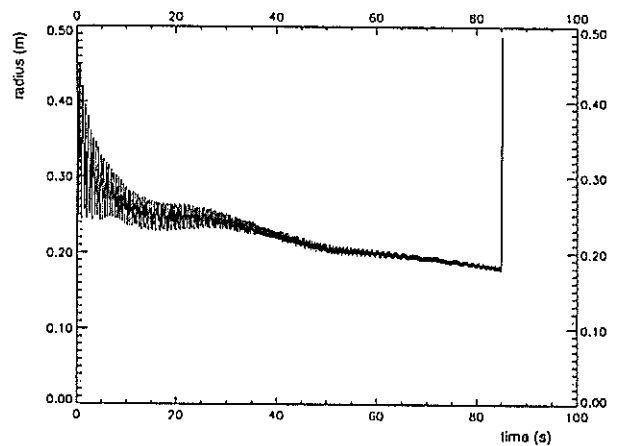


Fig. 6 Slug radius evolution, no viscous friction, tank radius 0.61 m

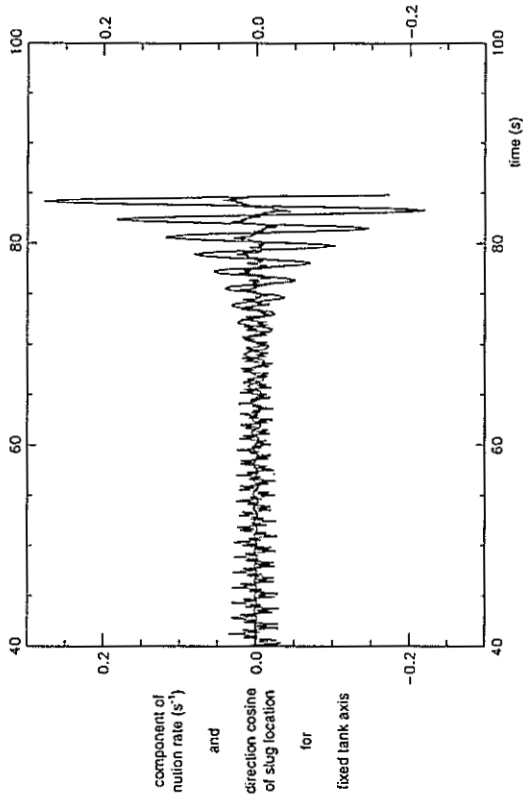


Fig. 8 Slug swirl frequency and tank nutation rate divergence for tank radius 0.41 m

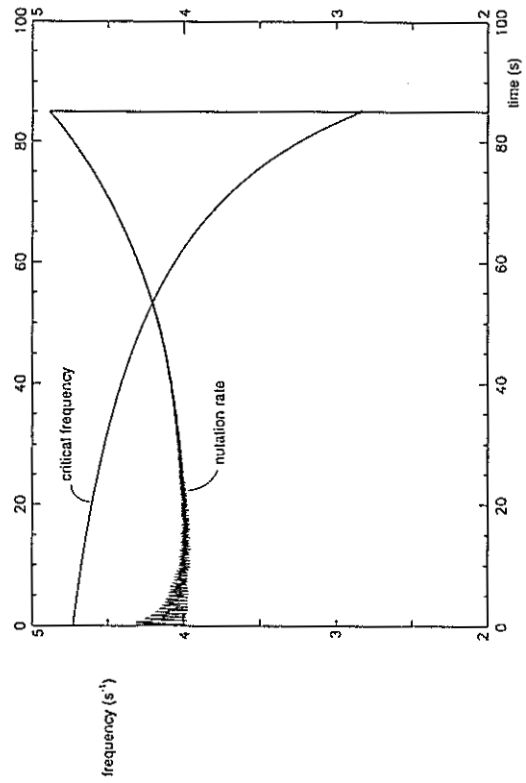


Fig. 10 PAM-D free nutation rate, and Poincaré stability condition for dumbbell

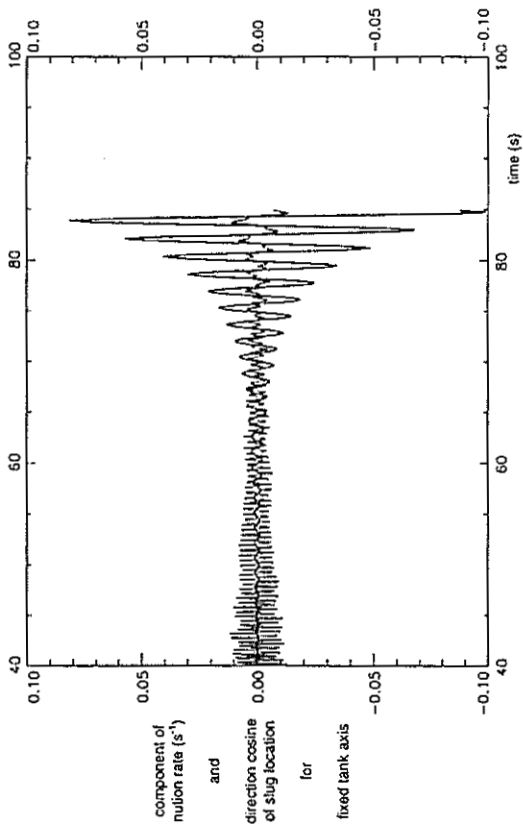


Fig. 7 Slug swirl frequency and tank nutation rate divergence for tank radius 0.61 m

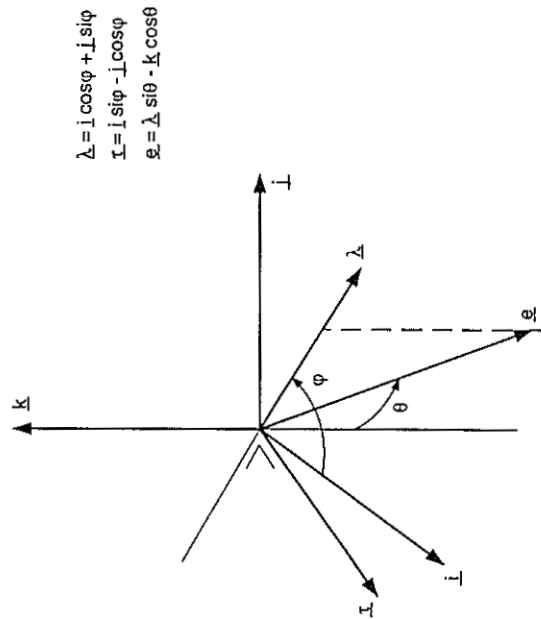


Fig. 9 Orientation of unit vector \underline{e}

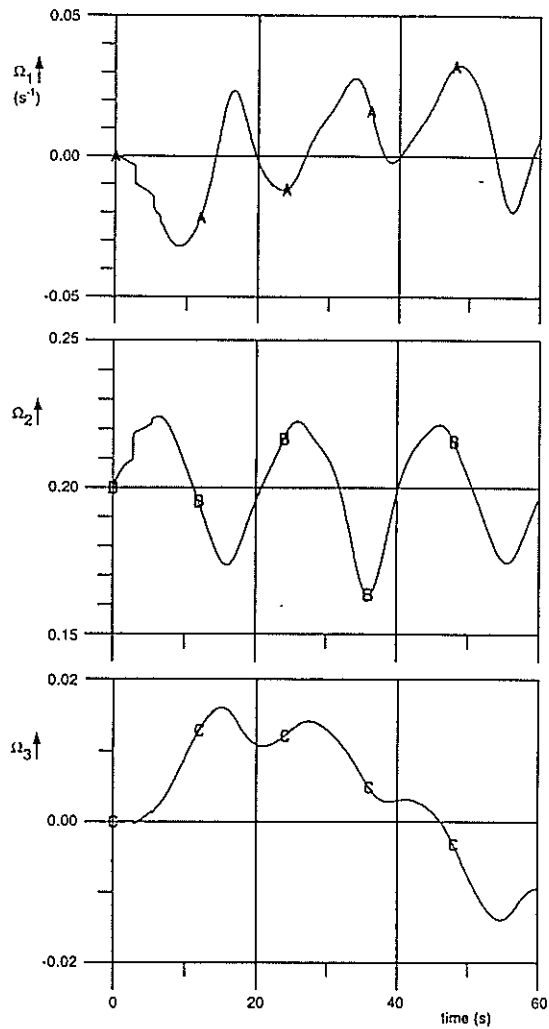


Fig. 11 Components of tank angular velocity during the uncontrolled evolution of Motion 1

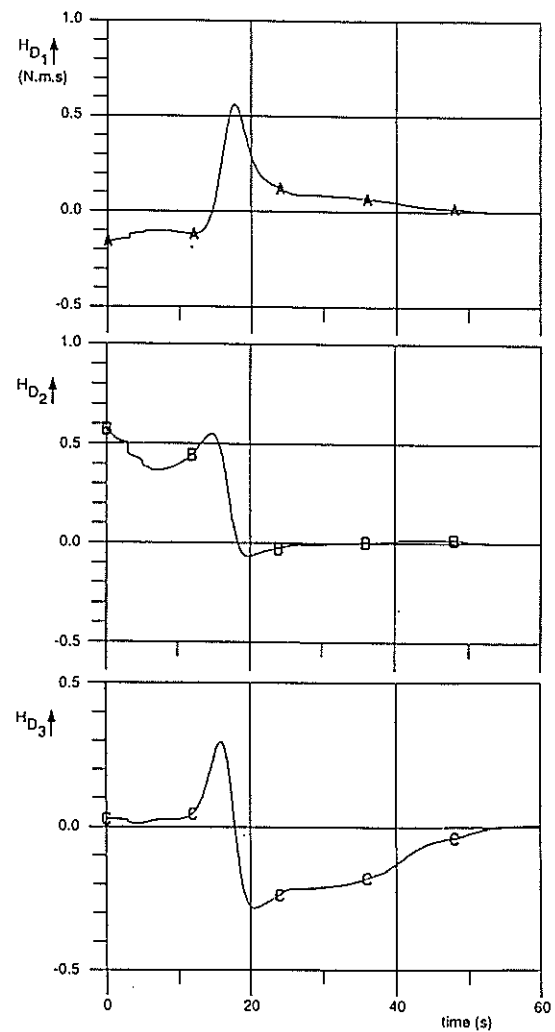


Fig. 12 Components of dumbbell angular momentum during control c-2

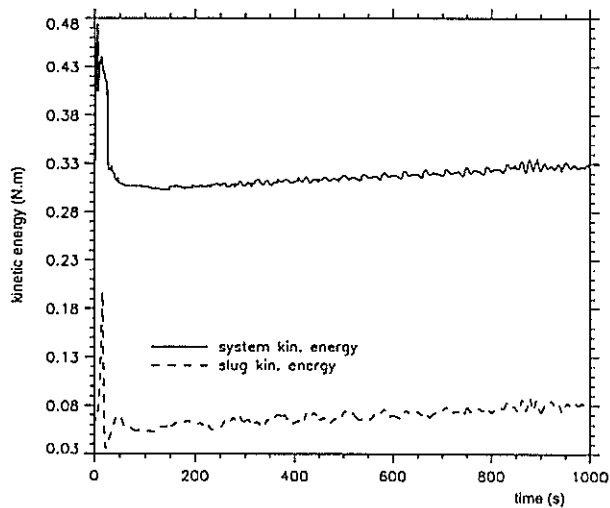


Fig. 13 Kinetic energy evolution with contact line friction, SMS control c-2

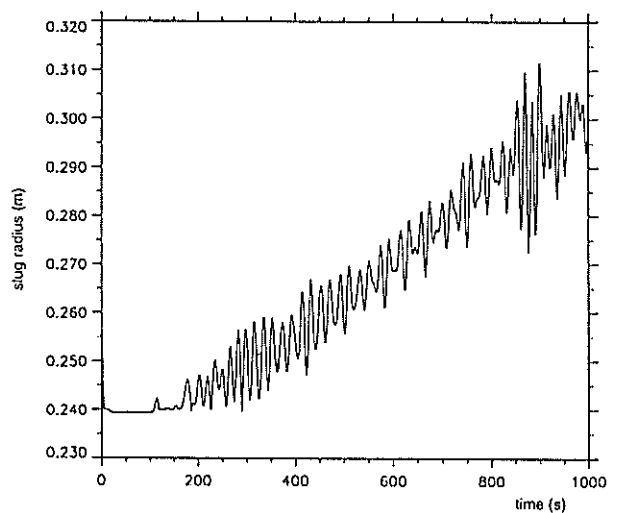


Fig. 14 Slug radius evolution with contact line friction, SMS control c-2